



## Modified Brittle Poly(lactic acid) by Biodegradable Hyperbranched Poly(ester amide)

Wei Zhang, Yu Zhang\*, and Yanmo Chen

State Key Laboratory for Modification of Chemical Fiber and Polymeric Materials  
College of Material Science and Engineering, Donghua University  
Shanghai-201620, PR China

Received 3 July 2008; accepted 30 November 2008

### ABSTRACT

Melt blending of poly(lactic acid) (PLA) and biodegradable hyperbranched poly(ester amide) (HBP) has been performed in order to toughen PLA without compromising its biodegradability and biocompatibility. The FTIR spectra, thermal properties, disperse phase morphology, and mechanical properties of the blends with different HBP contents were investigated. A reasonable toughening mechanism is also given. The presence of intermolecular hydrogen bonds between PLA and HBP is confirmed by FTIR spectroscopy technique. Addition of HBP not only reduced the crystallinity of PLA from 30.99% to 18.58%, but also has toughened it as well. By an increase in HBP content from 2.5% to 10%, the blend showed a slight increase in tensile strength but a significant increase in elongation-at-break values. Meanwhile the scanning electron micrographs showed an evenly dispersed HBP in PLA. The hydrogen bond interactions and the energy-dissipation process led to a tough biodegradable polymer blend.

### Key Words:

poly(lactic acid);  
biodegradable;  
hyperbranched poly(ester amide);  
blend;  
toughening.

### INTRODUCTION

Among many polymers, poly(lactic acid) (PLA) has been the most popular due to its high biocompatibility and biodegradability [1]. PLA is an aliphatic polyester derived from corn and sugar beets and degrades to non-toxic compounds in landfill. It can be synthesized either from direct condensation of lactic acid or

by ring-opening polymerization of the cyclic lactide dimer. PLA has been explored as a substitute for packaging film, thermoformed containers, short shelf-life bottles, food and non-food packaging materials, extruded foams, and other disposable items. But, its inherent brittleness and low tough-

(\*) To whom correspondence to be addressed.  
E-mail: [yzh@dhu.edu.cn](mailto:yzh@dhu.edu.cn)

ness have imposed constraints for PLA applications. In general, copolymerization and blending are the common methods to modify the brittleness of PLA. Blending is usually more practical and economically feasible for industrial use. Thus, substantial research works have been done on the blending of PLA with various polymers, such as poly(ether)urethane [2], poly(ethylene oxide) [3,4], poly( $\epsilon$ -caprolactone) [5], starch [6,7] and other polymers.

Hyperbranched polymer is a class of three-dimensional and artificially built molecules produced by multiplicative growth from small molecules. Hyperbranched polymers usually show low viscosities through high molecular weights, and as rheology modifiers are used to improve polymers melting fluidity [8]. Especially, hyperbranched polymers can provide a lot of terminal reactive chemical groups such as hydroxyl and carboxyl groups and behave as surface modifying agents or toughening additives [9-11]. Introducing hydrogen bond interactions has proved an effective method to improve the toughness of the polymers. Fei et al. [12,13] obtained PHBV with high toughness modified by 4,4'-dihydroxydiphenyl propane using hydrogen bonding. Hydroxyl groups are seemed to be as effective proton donors and easily enter hydrogen bonding interactions with C=O groups of aliphatic polyesters. Hyperbranched polymers with abundant hydroxyl end groups in PLA may be employed to enhance the mechanical properties of the matrix by molecular interactions. In addition, many research works have been made to reduce the crystallinity of polymers in order to make them ductile [14]. The potential interaction between hyperbranched polymers and PLA matrix may constrain the mobility of PLA macromolecules and therefore would reduce the crystallinity of PLA.

In this article, we report a novel modification method by using biodegradable hyperbranched poly(ester amide) to improve the toughness of PLA. FTIR spectra were performed to prove the hydrogen bond between HBP and PLA molecules. Up to the present, according to our knowledge, there is limited literature about hydrogen bonding between HBP and PLA molecules. The thermal properties of the blend and dispersion of HBP in PLA are studied by DSC, TGA and SEM techniques. The influence of hyperbranched polymer and its content on mechanical

properties of PLA are studied as well.

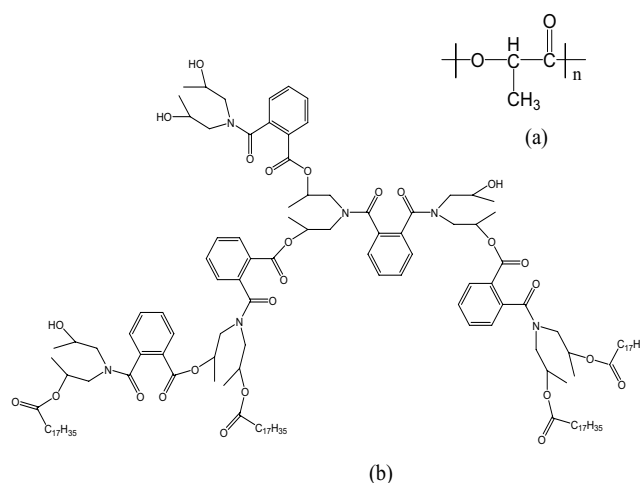
## EXPERIMENTAL

### Materials

PLA was supplied by Bright China Industrial Co. Ltd. (Shenzhen, China). Its average molecular weight was measured by viscosity in chloroform and yielded  $M_w = 1.0 \times 10^5$  g/mol. The biodegradable hyperbranched polymer (HBP) was donated by DSM corporation (Heerlen, Netherlands), having the trade name HYBRANE PS2550. Its average molecular weight was about 2500 g/mol with a hydroxyl number of 90-110 mg KOH/g and maximum acid number of 4 mg KOH/g. The chemical structures of PLA and HYBRANE PS2550 are presented in Scheme I.

### Preparation of PLA and HBP Blends

Before blending, the PLA and HBP were dried at 70°C and at 40°C for 24 h in vacuum oven, respectively. The blends were prepared by melt mixing in a microcompounder (Haake RC90, Germany). Polymers were mixed at screw speed of 50 rpm for 5 min at 170°C. PLA was mixed with HBP from 2.5 to 20% (w/w). Also, the neat PLA was subjected to the mixing treatment for undergoing the same thermal history as the blend. In this work, we use the term 'Hn' to represent the blend containing n% HBP, such as H10 that means the blend containing 10% HBP and 90% PLA.



**Scheme I.** Chemical structure of (a) PLA and (b) HYBRANE PS2550.

## Characterization

### FTIR Spectroscopy

FTIR spectra were recorded at  $4\text{ cm}^{-1}$  resolution on Nicolet Nexus-670 FTIR spectrophotometer in the range of  $500\text{--}4000\text{ cm}^{-1}$ . Typically 64 spectra were signal-averaged to reduce spectral noise. The chloroform solutions containing the blend samples were cast each onto a conventional KBr disk and allowed to evaporate at room temperature followed by drying at  $40^\circ\text{C}$  for 24 h in a vacuum oven.

### DSC Analysis

DSC measurements of blends were carried out on a DSC822e Mettler-Toledo, Switzerland. These measurements were performed in nitrogen atmosphere at heating and cooling rates of  $10^\circ\text{C}/\text{min}$ . The samples were heated from  $-20^\circ\text{C}$  to  $140^\circ\text{C}$ , holding for 5 min to erase thermal history effects and cooled to  $-20^\circ\text{C}$  then heated to  $200^\circ\text{C}$  again for the second scan. All the data were collected by the second scan. The degree of crystallinity of the samples were calculated from the ratio of their enthalpy of fusion to the enthalpy of fusion of the PLA crystal with a value of  $H_m = 93\text{ J/g}$ .

### TGA Analysis

TGA measurements were performed with a NETZSCH TG-209-F1 thermogravimetric analyzer. Conventional TGA measurements at constant heating rate were run at  $10^\circ\text{C}/\text{min}$  in nitrogen with the sample size about 8-10 mg to provide a control set values for thermal decomposition parameters. The nitrogen flow was  $30\text{ mL}/\text{min}$ .

### SEM

SEM studies were carried out with a JSM-5600 LV scanning electron microscope (Jeol, Japan). The samples were broken into pieces in liquid nitrogen and then were etched in ethanol for 24 h to dissolve the HBP phase selectively, followed by vacuum drying at  $40^\circ\text{C}$  for 12 h. All samples were sputtered with gold and observed under a working voltage of 10 kV. The magnification is indicated in the photos.

### Mechanical Testing

Tension properties were determined using a screw-driven universal testing machine. Tensile bars were hot injection-moulded at  $170^\circ\text{C}$ , 5 MPa for 3 min by a

DAKA instrument, and then cooled to room temperature under ambient condition. Test conditions were as follows:

Temperature:  $25^\circ\text{C}$ , gauge length: 30 mm, and crosshead speed:  $5\text{ mm}/\text{min}$ . All the data reported were mean values and standard deviations are calculated from five sets of data.

## RESULTS AND DISCUSSION

### FTIR Analysis

The FTIR spectra of pure PLA, HBP, and their blends with different contents are given in Figure 1. In the FTIR spectra of PLA, the peaks can be observed at  $1759\text{ cm}^{-1}$  corresponding to  $\text{--C=O}$  stretching vibration;  $1089\text{ cm}^{-1}$  corresponding to the  $\text{--C--O--}$  stretching vibration;  $1456\text{ cm}^{-1}$  corresponding to the  $\text{--CH}_3$  bending vibration;  $2997\text{ cm}^{-1}$  and  $2946\text{ cm}^{-1}$  corresponding to the  $\text{--CH}_2\text{--}$  asymmetric and symmetric stretching vibrations. The intensity of the signals of the absorption bands centered at  $2921\text{ cm}^{-1}$  and  $2852\text{ cm}^{-1}$  were assigned to the  $\text{--CH}_2\text{--}$  stretching vibration of stearic acid group, and centered at  $1641\text{ cm}^{-1}$  were assigned to the  $\text{--CON<}$  bending vibration of the amide group in the HBP spectra. Meanwhile, the absorbance intensity of hydroxyl groups (in the region  $3500\text{--}3300\text{ cm}^{-1}$ ) increased as well. In FTIR

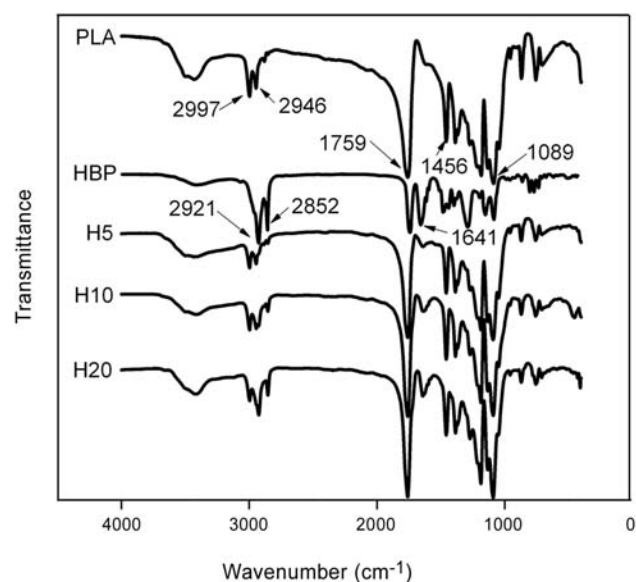


**Figure 1.** FTIR spectra of HBP/PLA blends at different contents.

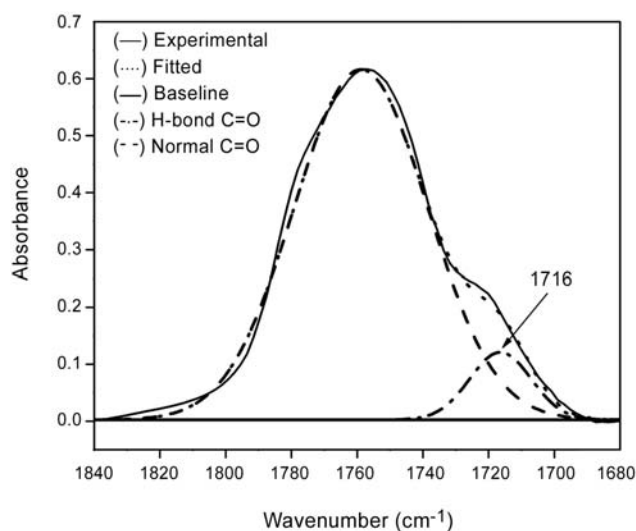


**Figure 2.** Experimental and fitted  $-C=O$  absorption in FTIR spectra of the H20 blend.

spectra of H5, H10 and H20, the characteristic peaks of PLA and HBP were observed the same, indicating that the HBP/PLA blends had all expected characteristic groups and were prepared successfully.

In HBP, the  $-OH$  groups showed a strong preference to act as proton donor. Thus, it is easy to interact with  $-C=O$  groups of PLA by hydrogen bonds. The FTIR results exhibited that an obvious signal appeared at about  $1716\text{ cm}^{-1}$  when the HBP content is 20%, and the intensity increased with the increase of HBP content. The absorbance at  $1716\text{ cm}^{-1}$  should be assigned to the hydrogen bonded  $-C=O$  groups [13]. The absorbance intensity increased with increase of H-bonded  $-C=O$  groups by higher HBP content. The FTIR curves of  $-C=O$  absorptions of all HBP/PLA blends were fitted by Gaussian function. As an example, the experimental and fitted  $-C=O$

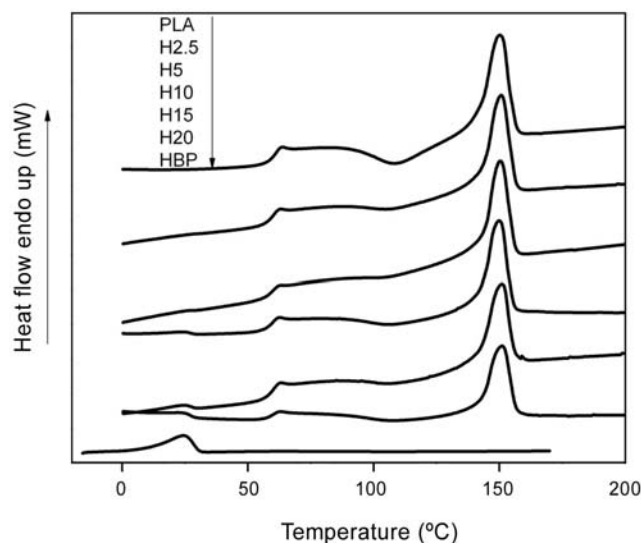


**Figure 3.** DSC traces of HBP/PLA blends at various concentrations.

absorptions in FTIR spectra of the H20 blend are shown in Figure 2. The experimental and fitted curves were perfectly consistent which indicated the reliability of the curve-fitting technique. The main peak at  $1759\text{ cm}^{-1}$  is attributed to the normal  $-C=O$  groups of PLA. The other small peak at  $1716\text{ cm}^{-1}$  should be assigned to the H-bonded  $-C=O$  groups. It can be concluded that there are intermolecular hydrogen bonds between PLA and HBP.

### Thermal Properties

DSC measurement was employed to evaluate the thermal properties of PLA, HBP, and HBP/PLA blends with various concentrations. Figure 3 shows the second heating scans at a rate of  $10^\circ\text{C}/\text{min}$  and the results obtained from these heating scans for all samples are listed in Table 1. When the HBP contents

**Table 1.** Thermal properties of blends with various HBP contents.

Samples	$T_{g1}$ ( $^\circ\text{C}$ )	$T_{g2}$ ( $^\circ\text{C}$ )	$T_m$ ( $^\circ\text{C}$ )	$T_{d1}$ ( $^\circ\text{C}$ )	$T_{d2}$ ( $^\circ\text{C}$ )	$H_c$ (J/g)	$H_m$ (J/g)	$X_c$ (%)
PLA	63.60	-	150.11	358.01	-	7.50	28.82	30.99
H2.5	62.37	-	150.12	359.02	-	5.55	24.87	26.71
H5	61.91	-	150.37	356.92	-	4.60	23.82	25.61
H10	61.94	24.63	149.80	357.87	-	3.82	19.36	20.82
H15	61.93	24.29	150.14	350.36	304.49	2.95	18.85	20.27
H20	61.95	24.30	151.17	348.41	314.26	2.91	17.28	18.58
HBP	-	23.58	-	-	301.00	-	-	-

were below 5%, the samples showed only one single  $T_g$ , and the  $T_g$  decreased slightly with increase in HBP content, such as  $T_{g(PLA)} = 63.60$ ,  $T_{g(H2.5)} = 62.37^\circ\text{C}$ , and  $T_{g(H5)} = 61.91^\circ\text{C}$ . In contrast, the samples showed two  $T_g$  points, when the HBP content was higher than 10%. For example, the  $T_{g1}$  and  $T_{g2}$  of the H10 are shown to be  $61.94^\circ\text{C}$  and  $24.63^\circ\text{C}$ , respectively, indicating the partial miscibility of the polymer blends.

Crystallization properties have strong influence on mechanical properties and degradation rate of PLA. Therefore, the influence of HBP on crystallization behaviour of PLA was investigated and shown in Figure 3. The DSC trace of pure PLA has exhibited a large exothermic peak compared to HBP/PLA blends at  $108^\circ\text{C}$ . All the samples have shown a tiny broad exothermic peak at about  $100\text{--}120^\circ\text{C}$  and the crystallization area has decreased with higher HBP contents. As it is shown in Table 1 the crystallinity is lowered from 30.99% for pure PLA to 18.58% for H20. It may be concluded that the HBP has reduced the crystallinity of PLA. The reason can be explained by two inter-related factors:

Firstly, the interaction between PLA and HBP by hydrogen bond constrains the mobility of PLA molecules. Secondly, the dilution effect of the amorphous phase of HBP on the system decreases the crystallinity of each blend.

TGA curves of HBP/PLA blends of various contents at the heating rate of  $10^\circ\text{C}/\text{min}$  in nitrogen stream are shown in Figure 4a. The decomposition temperature ( $T_d$ ) moved to lower temperature while the HBP content has been increased. The derivative thermogravimetric (DTG) curves of the HBP/PLA blends of various contents are shown in Figure 4b. Here  $T_d$  is the temperature at the maximum rate of weight loss, that is, the decomposition temperature. The  $T_d$  of pure PLA and HBP is  $358^\circ\text{C}$  and  $301^\circ\text{C}$ , respectively. The presence of a single peak in the DTG curves of the blends with 2.5%–10% HBP contents suggests that weight loss has occurred in a single stage and their  $T_d$  point is at about  $358 \pm 2^\circ\text{C}$ . This behaviour is attributed to the high dispersion and partial miscibility of HBP and PLA in blends. But when the HBP contents were above 15%, the blends showed obviously two peaks. The  $T_{d1}$  of PLA in formulations H15 and H20 decreased in comparison with pure

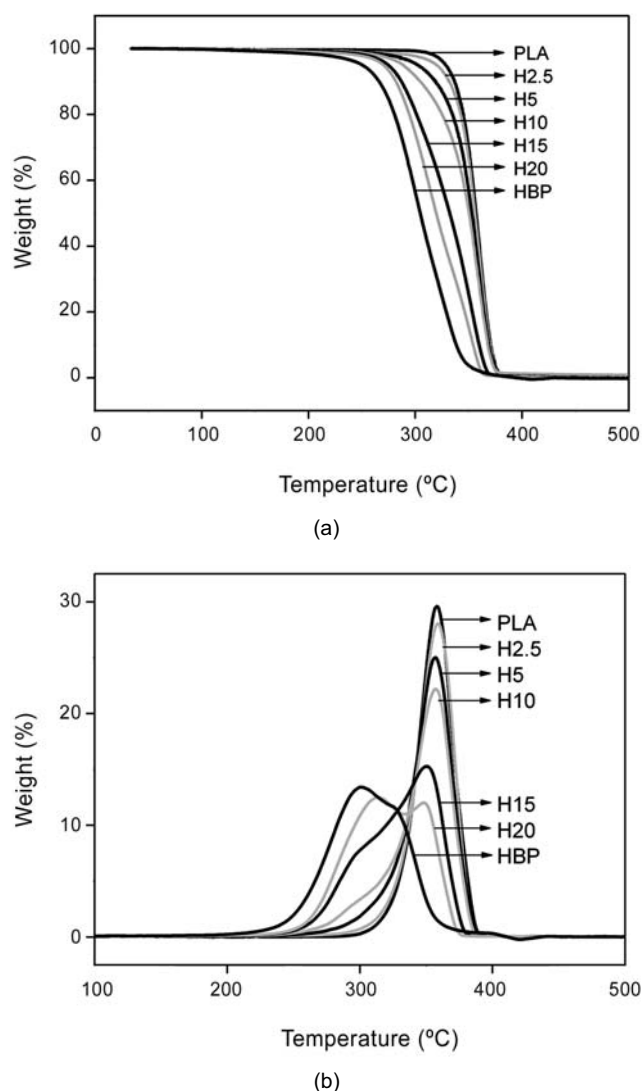


**Figure 4.** (a) TGA curves of HBP/PLA blends of various contents at heating rate of  $10^\circ\text{C}/\text{min}$ . (b) DTG curves of HBP/PLA blends of various contents at heating rate  $10^\circ\text{C}/\text{min}$ .

PLA, which could be an indication that the HBP possibly has facilitated the thermal decomposition of PLA.

### Disperse Phase Morphology

The mechanical properties of materials are dependent on the phase structure. Figure 5 represents the scanning electron micrographs of the HBP/PLA blends with various HBP contents. As shown in Figure 5a, the surface of pure PLA is completely flat, which is an indication of the brittle failure in PLA. The Figure 5b shows the surface of H2.5 blend. There are few small cavities on the surface which is slightly coarse

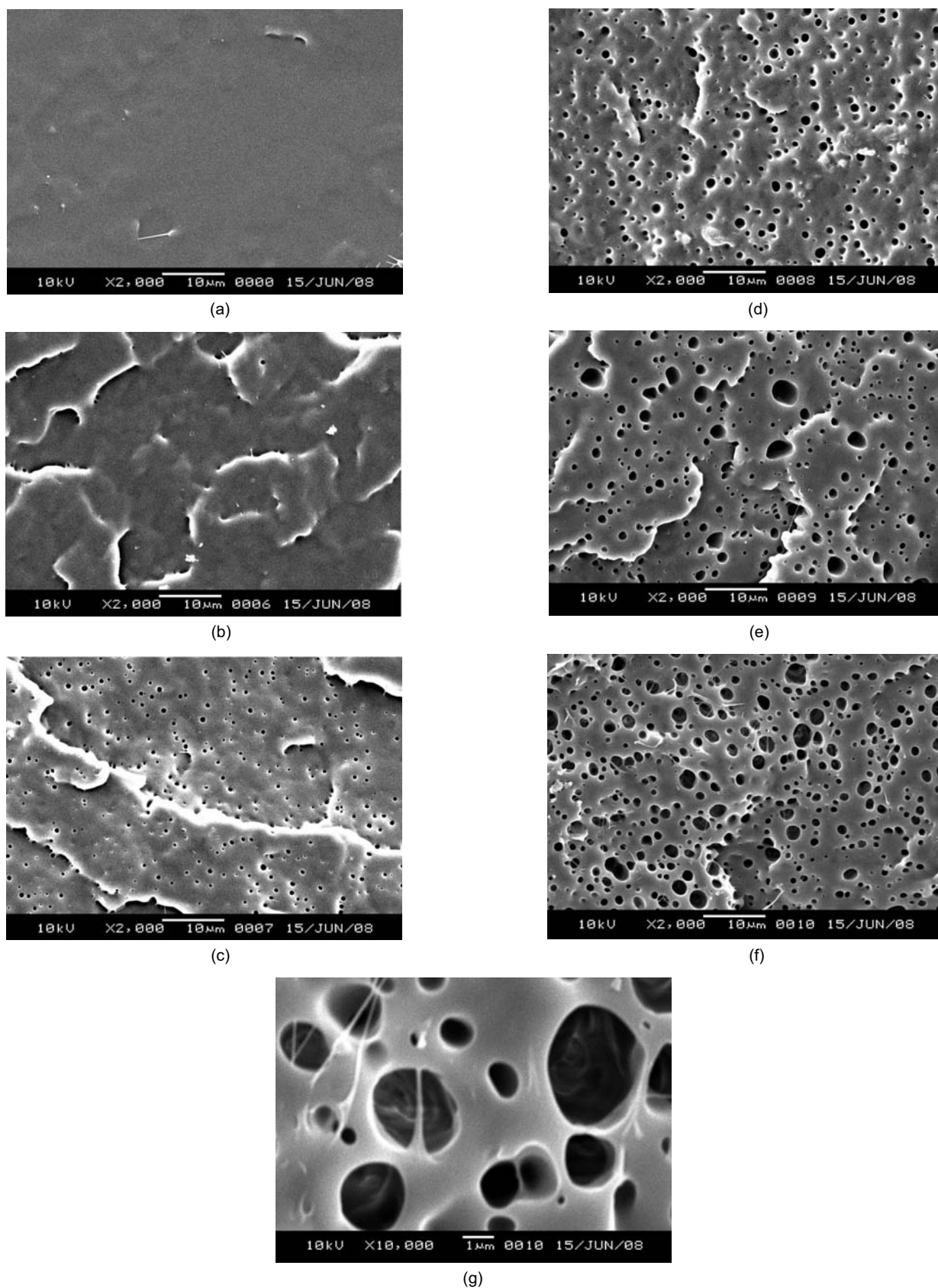


**Figure 5.** Phase morphologies of the HBP/PLA blends of various contents: (a) pure PLA, (b) H2.5, (c) H5, (d) H10, (e) H15, (f) H20, and (g) H20 (magnifications, a-f:  $\times 2000$  and g:  $\times 10000$ ).

compared to pure PLA. This proves that the HBP is equally dispersed into PLA matrix, which is made slightly ductile. When HBP content is above 5%, the small cavities are observed in Figure 5c. The size of cavities shows narrow distribution, and the diameter of cavities is almost 0.3-0.6  $\mu\text{m}$ .

Continuing to increase the HBP content to 10% level, the size of the cavities has increased to 0.5-1  $\mu\text{m}$  as shown in Figure 5d. When the HBP content is higher than 15%, the size distribution of the cavities is within a wide diameter range of 1-4  $\mu\text{m}$ , such as shown in Figures 5e and 5f. Especially in H20 blend, the cavities are adjacent or consecutive which means the HBP domains are partially connective in the matrix as shown in Figure 5g with  $10^4$  magnifications.

### Tensile Properties

Stress-strain curves of neat PLA and HBP/PLA blends are shown in Figure 6a, while the tensile strength and elongation-at-break curves are shown in Figure 6b. It is observed that addition of HBP has changed the tensile properties of PLA significantly. Pure PLA is very rigid and brittle. The tensile strength of pure PLA is 46.58 MPa and the elongation-at-break is only 5% with no yield point. On the contrary, the HBP/PLA blends have shown obvious ductile fracture. The tensile strength of the blends has increased from 48.31 MPa to 53.17 MPa, according to respective 2.5% and 5% HBP contents. Meanwhile, the elongation-at-break has increased from 12.11% to 24.01%. When HBP content is above 10%, its tensile strength has decreased to 48.81 MPa, but its elongation-at-break has increased to the maximum value of 43.06%. The H5 and H10 blends show yielding and stable neck growth under tensile load. It is proved that HBP has toughened the PLA. Its toughening mechanism may be explained by the following arguments. At first, the hydrogen bond interactions between HBP and PLA enhance the interfacial adhesion and improve the mechanical properties of the blends [13]. Secondly, PLA with lower crystallinity becomes more ductile. Thirdly, the HBP domains act as stress concentrators upon being subjected to the tensile test which is an important energy-dissipation process and leads to the toughening of PLA [2].

When the content of HBP is above 15%, the

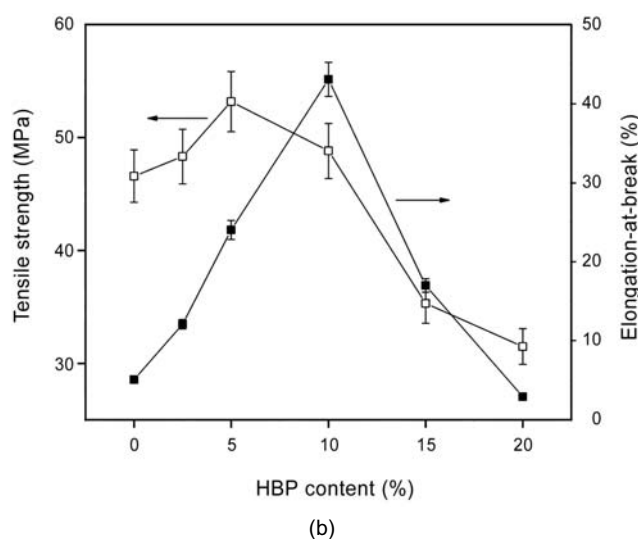
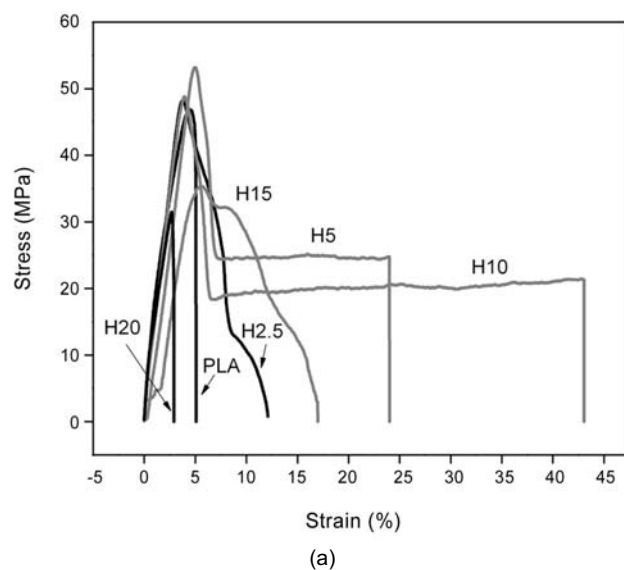


**Figure 6.** (a) Stress-strain curves of the HBP/PLA blends with different HBP contents. (b) Tensile strength and the elongation-at-break of HBP/PLA blends with different HBP contents.

mechanical properties of the blend have sharply dropped. The tensile strengths of H15 and H20 are 35.32 MPa and 31.49 MPa, while the elongation-at-breaks of H15 and H20 are 17.00% and 2.92% respectively. It is because HBP has shown lower tensile strength and elongation-at-break than PLA. When the HBP content is lower than 10%, the hydrogen bond interaction enhances the interfacial adhesion leading to a better tensile strength. But with the HBP increase, the HBP phase shows cavities with a wide distribution of size and diameter. This may be explained by the fact that steric hindrance and dilution effects have

become dominant and the blends beyond 15% HBP show lower tensile strength and elongation-at-break values.

## CONCLUSION

A series of HBP/PLA blends have been successfully prepared by melt blending. It is found that the addition of HBP significantly improves the mechanical properties of PLA. The tensile strength and elongation-at-break of the blends increase with the increases in HBP content. Especially, the blend with 10% HBP shows good tensile strength of about 48.81 MPa, and wonderful elongation-at-break of about 43.06%, compared to pure PLA. The experimental results have indicated that the improvement of mechanical properties is due to the hydrogen bond interactions between PLA and HBP, and the energy-dissipation process. We believe that the method of toughening shows good prospects in expanding the application of the PLA such as shape memory materials, body replacement materials, etc.

## REFERENCES

1. Gross RA, Kalra B, Biodegradable polymers for the environment, *Science*, **297**, 803-807, 2002.
2. Li YJ, Shimizu H, Toughening of polylactide by melt blending with a biodegradable poly(ether) urethane elastomer, *Macromol BioSci*, **7**, 921-928, 2007.
3. Yasuyuki A, Kiyofumi S, Yosikazu K, Ryoki N, Preparation and properties of the biodegradable graded blend of poly(L-lactic acid) and poly(ethylene oxide), *J Polym Sci Polym Phys*, **45**, 2972-2981, 2007.
4. Gaikwad AN, Wood ER, Ngai T, Lodge TP, Two calorimetric glass transitions in miscible blends containing poly(ethylene oxide), *Macromolecules*, **41**, 2502-2508, 2008.
5. Takeshi S, Kazuo K, Umaru SI, Masaya K, Hiroyuki H, Effect of compounding procedure on mechanical properties and dispersed phase morphology of poly(lactic acid)/polycaprolactone blends containing peroxide, *J Appl Polym Sci*, **103**, 1066-1074, 2007.
6. Wang N, Yu J, Ma XF, Preparation and characterization of compatible thermoplastic dry starch/poly(lactic acid), *Polym Compos*, **29**, 551-559, 2008.
7. Ke T, Sun X, Thermal and mechanical properties of poly(lactic acid) and starch blends with various plasticizers, *T Asae*, **44**, 945-953, 2001.
8. Diao JZ, Yang HF, Zhang JM, Song XH, Preparation and characterization of PP and PP-g-(MAH-co-St)/hyperbranched poly(amide-ester) blends, *Iran Polym J*, **16**, 97-104, 2007.
9. Bhardwaj R, Mohanty AK, Modification of brittle polylactide by novel hyperbranched polymer-based nanostructures, *Biomacromolecules*, **9**, 758-758, 2008.
10. Zhang JF, Sun XZ, Mechanical properties and crystallization behavior of poly(lactic acid) blended with dendritic hyperbranched polymer, *Polym Int*, **53**, 716-722, 2004.
11. Wong S, Shanks AR, Hodzic A, Mechanical behavior and fracture toughness of poly(L-lactic acid)-natural fiber composites modified with hyperbranched polymers, *Macromol Mater Eng*, **289**, 447-456, 2004.
12. Fei B, Chen C, Wu H, Peng SW, Wang XY, Dong LS, Quantitative FTIR study of PHBV/bisphenol A blends, *Eur Polym J*, **39**, 1939-1946, 2003.
13. Fei B, Chen C, Wu H, Peng SW, Wang XY, Dong LS, Xin HJ, Modified poly(3-hydroxybutyrate-co-3-hydroxyvalerate) using hydrogen bonding monomers, *Polymer*, **45**, 6275-6284, 2004.
14. Bahari K, Mitomo H, Enjoji T, Hasegawa S, Yoshii F, Makuuchi K, Radiation-induced graft polymerization of styrene onto poly(3-hydroxybutyrate) and its copolymer with 3-hydroxyvalerate, *Angew Makromol Chem*, **250**, 31-44, 1997.